Robotica: (2019) volume 37, pp. 1582–1594. © Cambridge University Press 2019
doi:10.1017/S0263574719000158

Monocular Vision-based Sense and Avoid of UAV Using Nonlinear Model Predictive Control

Yizhai Zhang†, Wenhui Wang†, Panfeng Huang†*, Zainan Jiang‡*

† *Research Center of Intelligent Robotics, School of Astronautics, Northwestern Polytechnical University, Xi'an, Shaanxi, 710072, China. E-mails: zhangyizhai@nwpu.edu.cn, wenhuiwang024@mail.nwpu.edu.cn*
‡ *State Key Laboratory of Robotics and System, Harbin Institute of Technology, Harbin, Heilongjiang, 150080, China*

(Accepted January 19, 2019. First published online: March 6, 2019)

SUMMARY
The potential use of onboard vision sensors (e.g., cameras) has long been recognized for the Sense and Avoid (SAA) of unmanned aerial vehicles (UAVs), especially for micro UAVs with limited payload capacity. However, vision-based SAA for UAVs is extremely challenging because vision sensors usually have limitations on accurate distance information measuring. In this paper, we propose a monocular vision-based UAV SAA approach. Within the approach, the host UAV can accurately and efficiently avoid a noncooperative intruder only through angle measurements and perform maneuvers for optimal tradeoff among target motion estimation, intruder avoidance, and trajectory tracking. We realize this feature by explicitly integrating a target tracking filter into a nonlinear model predictive controller. The effectiveness of the proposed approach is verified through extensive simulations.

KEYWORDS: Aerial robotics; Navigation; Control of robotic systems; Sense and avoid; Obstacle avoidance.

1. Introduction

Unmanned aerial vehicles (UAVs) have become a promising mobile platform for commercial and civilian applications,[1] such as surveillance, aerial photography, and search and rescue. However, the use of UAVs further increases civilian airspace density, which is already crowded by manned aircrafts. In order to guarantee safety, one noteworthy technical trend is the integration of UAVs into the current national airspace system. Thus, the Sense and Avoid (SAA) is considered as a critical function of UAVs in leveraging their full potentials.[2,3] For SAA, the UAVs not only are capable of detecting potential collision objects, but also need to perform effective collision avoidance maneuvers (see Fig. 1).

Many SAA prototypes and approaches have been reported recently.[4–6] Reference [7] outlines and reviews the substantial breadth of SAA architectures, technologies, and algorithms. Reference [6] provides an in-depth discussion on SAA progress related to fundamental components of sensing techniques, decision making, path planning, and path following. In all SAA studies, onboard devices and sensors play an important role in detecting, tracking, and avoiding intruders. Some SAA solutions use cooperative sensors, such as Traffic Collision Avoidance System[8] and Automatic Dependent Surveillance-Broadcast.[9] Others adopt noncooperative methods depending on radar,[10–12]

* Panfeng Huang and Zainan Jiang are both corresponding authors. E-mails: pfhuang@nwpu.edu.cn, jiangzainan@hit.edu.cn

https://doi.org/10.1017/S0263574719000158 Published online by Cambridge University Press

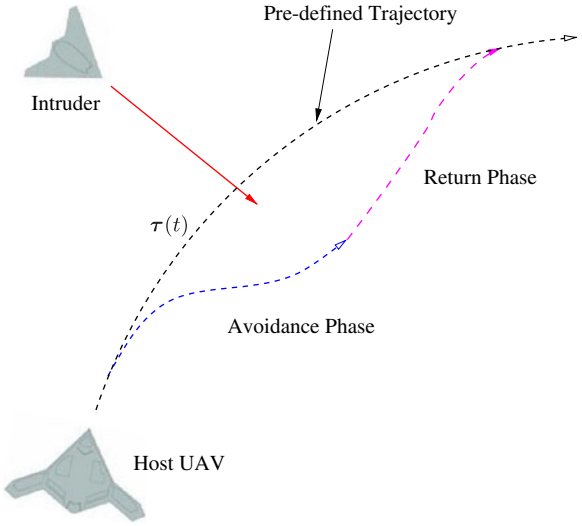


Fig. 1. Diagram of one SAA maneuver.

Light Detection And Ranging,[13–15] and vision sensors (e.g., cameras).[16] Cooperative sensors usually cannot be used for noncooperative intruders because the intruder does not equip same devices and the communication between the host UAV and intruder is also impossible. For noncooperative methods, vision sensors offer advantages over other sensors as they are low cost and lightweight but provide rich perception information.[17–19] Such features are more attractive for micro UAVs that have limited payload capacity and are sensitive to manufacturing costs.

Although the potential of vision sensors has already been recognized, vision-based SAA for UAVs is however challenging. First, the environmental awareness and intruder detection using onboard vision sensors are not trivial. SAA maneuvers are often performed under middle-distance (a few kilometers) or even long-distance conditions (up to tens of kilometers) to guarantee sufficient safety allowances. The intruder therefore appears small and dim on the imaging plane of vision sensor. In addition, the airborne environment is always complicated and highly unpredictable, for example, the constantly changing light condition.[20] Second and more importantly, monocular vision provides only incomplete information and has the well-known limitation in measuring the relative distance between the host UAV and intruder.[6] Although binocular vision can solve the distance missing problem, it is not suitable for UAV SAA considering the limited baseline of UAV and large SAA operation range.

Many SAA planning and control schemes have been proposed and validated.[21,22] In ref. [21], a dynamic path planning method of UAV was presented to avoid not only static threats but also mobile threats. In ref. [22], a collision-free guidance control system was designed by using nonlinear model predictive control (NMPC) for small unmanned helicopters and the collision avoidance was regarded as a state constraint in controller design. In ref. [23], a feasible three-dimensional collision avoidance course is on-line calculated for fixed-wing UAVs by keeping relative bearing and elevation angles. It is straightforward to know that all these SAA planning and control schemes assume that three-dimensional relative position between the host UAV and intruder can be accurately measured. Therefore, these approaches cannot be readily used for vision-based UAV SAA due to the lack of distance information.

In recent years, researchers have explored approaches to solve the distance missing problem in vision-based SAA. The essence of vision-based SAA is about angles-only navigation and control. In ref. [23], a vision-based SAA approach was implemented by maintaining a constant relative angle between the host UAV and intruder. In ref. [24], a dynamic safety envelope was proposed to adjust the heading direction of host UAV and to avoid the use of distance information. These two methods may not be used under certain situations and have obvious application restrictions. Inspired by the target motion analysis problem that originated in sonar signal processing field, another more convincing solution for vision-based SAA is to first estimate and recover distance information or equivalent parameters (e.g., time-to-collision) through angle measurements by using target tracking filter, such as the studies in refs. [25–27]. In target tracking filter studies, it has been strictly proven that the relative distance between target and host platform can be estimated through angle measurements

https://doi.org/10.1017/S0263574719000158 Published online by Cambridge University Press

as long as the maneuver of host platform satisfies observability condition.[28] The detailed design techniques of target tracking filter are introduced in refs. [29, 30], and how to plan the maneuver of host platform for optimal estimation accuracy is discussed in ref. [31]. In the above-mentioned vision-based SAA studies built on target tracking filter,[25–27] the target tracking filter and avoiding controller are usually designed and implemented, separately. The estimation results of target tracking filter are used as inputs given to avoiding controller. This is a standard and straightforward framework for vision-based SAA, which many prototypes have adopted and validated. However, the filter estimation performance indeed highly depends on real flying trajectory of the host UAV. Conversely, the filter estimation results also affect the obstacle avoiding maneuver. In other words, the filter estimation performance and the avoiding control performance are actually coupled. This coupling mechanism is a common characteristic for all angles-only navigation and control problems. In order to achieve optimal performance, the filter-based estimation, the navigation, and control have to be integrated together. The standard framework has not considered such coupling effect because the UAV SAA is an emerging topic.

In this paper, we propose a monocular vision-based SAA approach for UAVs by integrating a target tracking filter into a nonlinear model predictive controller. In this approach, the filter estimation, navigation, and control are combined together. The host UAV can accurately and efficiently avoid a noncooperative intruder through only angle measurements and perform maneuvers for optimal trade-off among target motion estimation, intruder avoidance, and trajectory tracking. To the best of the authors' knowledge, no previous work has been reported to explicitly fuse the target tracking filter and avoidance controller in vision-based SAA studies.

The remainder of this paper is organized as follows. Section 2 presents the problem description and coordinate system definitions. Sections 3 and 4 discuss the detailed SAA designs in avoidance and return phases, respectively. Extensive simulations are used to validate the proposed approach in Section 5. Section 6 obtains concluding remarks.

2. Problem Description and Coordinate System Definition

Figure 1 presents the diagram of vision-based SAA. In the beginning, the host UAV follows a predefined trajectory (denoted by $\boldsymbol{\tau}(t)$). A forward looking monocular camera is mounted on the host UAV. A noncooperative intruder then flies and approaches the host UAV. Once the threat of the intruder is confirmed, the host UAV performs an avoidance maneuver immediately. After the threat is dismissed, the host UAV returns to the predefined trajectory and finishes SAA process. In this study, we focus on the planning and control of the host UAV in the avoidance and return phases.

Several assumptions are adopted in this study. First, since in reality the SAA is more necessary and important for objects that flies at same attitude, we focus on two-dimensional SAA study and assume that the host UAV and intrude are flying in the same horizontal plane. Second, the motions of the host UAV are measured accurately by its conventional navigation sensors, such as GPS/INS. Third, the vision sensing of intruder is already finished and the directional angle of the intruder with respect to the host UAV is the visual measurement. Fourth, wind influence is not considered.

An inertial frame is defined as $\mathcal{I}(O, X, Y)$ (Fig. 2). We assume the body coordinate frame of UAV is $\mathcal{H}(O_b, x_b, y_b)$ with the origin at the centroidal center of the host UAV and the x_b-axis pointing forward. The yaw angle $\varphi(t)$ denotes the rotation from $\mathcal{I}$ to $\mathcal{H}$ (Fig. 2). The directional angle of the intruder in $\mathcal{H}$ is defined as $\phi(t)$ and provided by the monocular camera. The forward velocity of the host UAV is denoted as $v_f(t)$.

3. Vision-Based SAA Approach in Avoidance Phase

In this section, we present the detailed designs of the monocular vision-based SAA approach in avoidance phase.

3.1. Host UAV kinematic model

In order to significantly reduce the computation complexity of optimization problem in NMPC and make the controller more practical, the host UAV maintains a constant forward ground speed in the avoidance phase and the speed is denoted as v_c, that is, $v_f(k) = v_c$, $k \in \mathbb{N}$ for the kth step in time. Thus, only the yaw angle $\varphi(k)$ of the host UAV is controlled to implement the avoidance maneuver. We use discrete-time notations for all variables in the rest of paper because discrete-time representations are required for NMPC optimization.

The velocity vector of the host UAV in $\mathcal{I}$ is denoted as $\boldsymbol{v}_h(k)$ and we have

https://doi.org/10.1017/S0263574719000158 Published online by Cambridge University Press

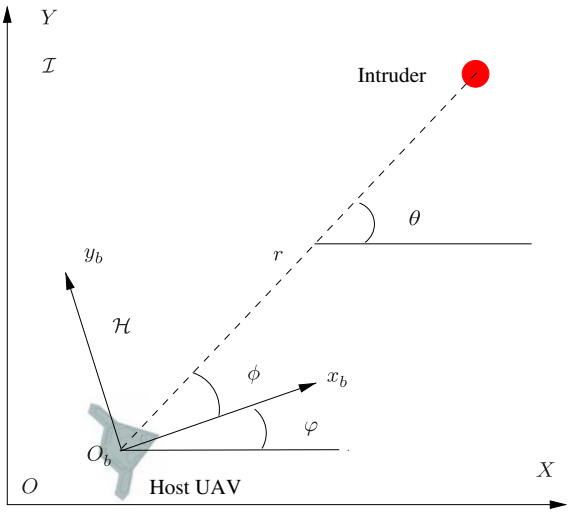


Fig. 2. Schematic of coordinate systems.

$$\boldsymbol{v}_h(k) = \begin{bmatrix} v_c \cos(\varphi(k)) \\ v_c \sin(\varphi(k)) \end{bmatrix}. \tag{1}$$

We then consider the angular velocity of $\varphi(k)$ as the virtual system input $u(k)$

$$u(k) = \dot{\varphi}(k). \tag{2}$$

Taking the derivative of (1) and plugging it into (2), we obtain the expression of acceleration vector of host UAV in $\mathcal{I}$

$$\boldsymbol{a}_h(k) = \begin{bmatrix} -\sin(\varphi(k)) \\ \cos(\varphi(k)) \end{bmatrix} v_c u(k). \tag{3}$$

We then define the state vector of host UAV in the avoidance phase as

$$\boldsymbol{x}_h(k) := [\boldsymbol{p}_h(k)^T \ \ \boldsymbol{v}_h(k)^T]^T \in \mathbb{R}^4, \tag{4}$$

where $\boldsymbol{p}_h(k) = [p_{hx} \ p_{hy}]^T \in \mathbb{R}^2$ and $\boldsymbol{v}_h(k) = [v_{hx} \ v_{hy}]^T \in \mathbb{R}^2$ are the position and velocity vectors, respectively. With (2) and (3), the kinematic model of the host UAV can be built as

$$\boldsymbol{x}_h(k+1) = \mathbf{A}\boldsymbol{x}_h(k) + \mathbf{B} \begin{bmatrix} -\sin(\varphi(k)) \\ \cos(\varphi(k)) \end{bmatrix} v_c u(k), \tag{5}$$

$$\varphi(k+1) = \varphi(k) + T u(k), \tag{6}$$

where T is the discrete sampling time, and matrices $\mathbf{A}$ and $\mathbf{B}$ are as follows

$$\mathbf{A} = \begin{bmatrix} 1 & 0 & T & 0 \\ 0 & 1 & 0 & T \\ 0 & 0 & 1 & 0 \\ 0 & 0 & 0 & 1] \end{bmatrix}, \quad \mathbf{B} = \begin{bmatrix} \frac{1}{2}T^2 & 0 \\ 0 & \frac{1}{2}T^2 \\ T & 0 \\ 0 & T \end{bmatrix}. \tag{7}$$

3.2. Intruder kinematic model

The intruder is assumed to be a noncooperative moving target that flies with a constant velocity. The position and velocity vectors of intruder are denoted as $\boldsymbol{p}_t(k) = [p_{tx} \ p_{ty}]^T \in \mathbb{R}^2$ and $\boldsymbol{v}_t(k) = [v_{tx} \ v_{ty}]^T \in \mathbb{R}^2$, respectively. We then define the state vector of the intruder as

$$\boldsymbol{x}_t(k) := [\boldsymbol{p}_t(k)^T \ \ \boldsymbol{v}_t(k)^T]^T \in \mathbb{R}^4. \tag{8}$$

It is straightforward to obtain the kinematic model of the intruder as

$$\boldsymbol{x}_t(k+1) = \mathbf{A}\boldsymbol{x}_t(k). \tag{9}$$

https://doi.org/10.1017/S0263574719000158 Published online by Cambridge University Press

Remark 1. The presented intruder kinematic model is just a guessed model to drive the following target tracking filter. In the SAA, the only external measurement for target tracking filter is bearing angle obtained from the vision sensor. In addition, the constant velocity assumption is not needed to be strictly satisfied because in filter design, the state model will include noise terms to compensate for system uncertainties.

3.3. Monocular vision-based relative motion estimation

A target tracking filter is used to estimate the relative motion between the intruder and the host UAV. Polar coordinate system has been shown more robust for relative motion estimation using only angle information.[30] We define a polar coordinate system with the origin coinciding with that of $\mathcal{H}$ and the polar axis paralleling the X-axis of $\mathcal{I}$ (Fig. 2). The relative target range and bearing angle of the intruder with respect to the host UAV are denoted as $r(k)$ and $\theta(k)$, respectively. As such, $\theta(k) = \varphi(k) + \phi(k)$ can be obtained by combining the measurements of the monocular camera and onboard navigation sensors. We then define the state vector of the intruder in the polar coordinate as

$$\boldsymbol{z}(k) = \begin{bmatrix} z_1(k) \\ z_2(k) \\ z_3(k) \\ z_4(k) \end{bmatrix} := \begin{bmatrix} \dot{\theta}(k) \\ \frac{\dot{r}}{r}(k) \\ \theta(k) \\ \frac{1}{r}(k) \end{bmatrix} \in \mathbb{R}^4. \tag{10}$$

For an intruder with a constant velocity (see (9)), the relative motion between the intruder and the host UAV can be modeled as[30]

$$\boldsymbol{z}(k+1) = \boldsymbol{z}(k) + T\,\boldsymbol{f}(k) + \boldsymbol{v}_f(k), \tag{11}$$

and

$$\boldsymbol{f}(k) = \begin{bmatrix} -2z_1z_2 + z_4(-a_{hx}(k)\cos(z_3) + a_{hy}(k)\sin(z_3)) \\ z_1^2 - z_2^2 + z_4(-a_{hx}(k)\sin(z_3) - a_{hy}(k)\cos(z_3)) \\ z_1 \\ -z_2z_4 \end{bmatrix}, \tag{12}$$

where $\boldsymbol{v}_f(k) \in \mathbb{R}^4$ represents the zero-mean white Gaussian noise for system uncertainties. Equation (11) can be considered system equations in the target tracking filter design. Because bearing angle $\theta(k)$ is the measurement, we define the measurement equation in target tracking filter design as

$$y(k) = \mathbf{H}\boldsymbol{z}(k) + v_h(k), \tag{13}$$

where

$$\mathbf{H} = \begin{bmatrix} 0 & 0 & 1 & 0 \end{bmatrix}. \tag{14}$$

In (13), $v_h(k)$ is the zero-mean white Gaussian noise for measurement uncertainties.

Any standard nonlinear filter design can be applied to (11) and (13). In this study, we adopt the extended Kalman filter (EKF) as an example because it is widely used in the aerospace field. The current estimate of the EKF for the kth step is defined as $\hat{\boldsymbol{z}}(k|k)$. The prediction and correction equations of the EKF are as follows:

$$\hat{\boldsymbol{z}}(k+1|k) = \hat{\boldsymbol{z}}(k|k) + T\,\boldsymbol{f}(k), \tag{15a}$$

$$\mathbf{P}(k+1|k) = \mathbf{F}(k)\mathbf{P}(k+1|k)\mathbf{F}^T(k) + \mathbf{Q}. \tag{15b}$$

$$\mathbf{W}(k+1) = \mathbf{P}(k+1|k)\mathbf{H}^T (\mathbf{H}\mathbf{P}(k+1|k)\mathbf{H}^T + R)^{-1} \tag{15c}$$

$$\hat{\boldsymbol{z}}(k+1|k+1) = \hat{\boldsymbol{z}}(k+1|k) + \mathbf{W}(k+1)[y(k+1) - \mathbf{H}\hat{\boldsymbol{z}}(k+1|k)] \tag{15d}$$

$$\mathbf{P}(k+1|k+1) = (\mathbf{I}_4 - \mathbf{W}(k+1)\mathbf{H})\mathbf{P}(k+1|k) \times (\mathbf{I}_4 - \mathbf{W}(k+1)\mathbf{H})^T + \mathbf{W}(k+1)\mathbf{R}\mathbf{W}^T(k). \tag{15e}$$

https://doi.org/10.1017/S0263574719000158 Published online by Cambridge University Press

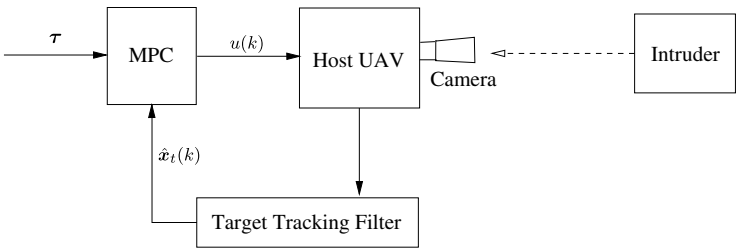


Fig. 3. Diagram of the proposed vision-based SAA approach.

In (15), $\mathbf{I}_4$ is the 4×4 identity matrix, $\mathbf{P}(k|k)$ is the error covariance matrix, $\mathbf{F}(k)$ is the Jacobian matrix of (11), and the details are shown in (16). $\mathbf{Q}$ and R are used to compensate for the system and measurement uncertainties.

$$\mathbf{F}(k) = \begin{bmatrix} -2x_2 & -2x_1 & x_4(a_{hy}\,\mathrm{s}_{x_3} + a_{hx}\,\mathrm{c}_{x_3}) & -a_{hy}\,\mathrm{c}_{x_3} + a_{hx}\,\mathrm{s}_{x_3} \\ -2x_1 & -2x_2 & x_4(a_{hy}\,\mathrm{c}_{x_3} + x_4 a_{hx}\,\mathrm{s}_{x_3}) & -a_{hy}\,\mathrm{s}_{x_3} + a_{hx}\,\mathrm{c}_{x_3} \\ 1 & 0 & 0 & 0 \\ 0 & -x_4 & 0 & -x_2 \end{bmatrix}. \tag{16}$$

Note that in the EKF, $\hat{\boldsymbol{z}}(k|k)$ and $\mathbf{P}(k|k)$ are expressed in polar coordinates. We need to transform the estimation results into $\mathcal{H}$ to facilitate the following controller design. Thus, we have

$$\hat{\boldsymbol{x}}_t(k) = \boldsymbol{x}_h(k) + \frac{1}{z_4}\begin{bmatrix} \sin(z_3) \\ \cos(z_3) \\ z_2\sin(z_3) + z_1\cos(z_3) \\ z_2\cos(z_3) - z_1\sin(z_3) \end{bmatrix}, \tag{17}$$

and

$$\mathbf{P}_{xy}(k) = \mathbf{F}(k)\mathbf{P}(k|k)\mathbf{F}(k)^T, \tag{18}$$

where $\hat{\boldsymbol{x}}_t(k) = [\hat{p}_{tx}\ \hat{p}_{ty}]^T$ is the estimated position vector of the intruder in $\mathcal{I}$ and $\mathbf{P}_{xy}(k)$ is the estimation error covariance matrix in Cartesian coordinate system.

3.4. NMPC-based SAA design

We use NMPC for SAA because of its attractive features on on-line optimization performance and constraint handling.[32,33] The diagram of the proposed SAA approach is presented in Figure 3. We assume the frequency of NMPC is the same as those of kinematic models and EKF, and define the length of the receding horizon window of NMPC as W. For clarity, all the predicted state variables are denoted in the receding horizon window with the sign $\tilde{}$, for example, $\tilde{\boldsymbol{x}}_h(k) = [\tilde{p}_{hx}\ \tilde{p}_{hy}]^T$, $\tilde{\boldsymbol{x}}_t(k) = [\tilde{p}_{tx}\ \tilde{p}_{ty}]^T$.

The goal of the SAA controller is to simultaneously obtain accurate estimates of intruder motion, avoid the intruder, and follow the predefined trajectory $\boldsymbol{\tau}(k)$. Therefore, the performance index of the SAA controller can be written as

$$J = \lambda_1\Phi(\tilde{\boldsymbol{x}}_h(k+N)) + \sum_{i=0}^{N-1}[L_1(\tilde{\boldsymbol{x}}_h(k+i)) + \lambda_2 L_2(\tilde{\boldsymbol{x}}_h(k+i))]. \tag{19}$$

The first cost term $\Phi(\tilde{\boldsymbol{x}}_h(k))$ is related to the EKF filter performance. In this study, $\Phi(\tilde{\boldsymbol{x}}_h(k))$ is designed to be the area of the predicted position uncertainty ellipse. Thus, we have

$$\Phi(\tilde{\boldsymbol{x}}_h(k)) = \pi\sqrt{(\det \mathbf{P}_{xy}(k))}. \tag{20}$$

Reducing this area $\Phi(\tilde{\boldsymbol{x}}_h(k))$ is equivalent to improving the filter estimation performance. $L_1(\tilde{\boldsymbol{x}}_h(k))$ is associated with the trajectory tracking performance and designed as

$$L_1(\tilde{\boldsymbol{x}}_h(k)) = |\tilde{\boldsymbol{x}}_h(k) - \boldsymbol{\tau}(k)|^2. \tag{21}$$

https://doi.org/10.1017/S0263574719000158 Published online by Cambridge University Press

$L_2(\tilde{\boldsymbol{x}}_h(k))$ is the penalty term related to the collision avoidance maneuver. To avoid the intruder, a prohibited circular area around the intruder is established as

$$g(\tilde{\boldsymbol{x}}_h(k)) = r_0^2 - [(\tilde{p}_{hx} - \hat{p}_{tx})^2 + (\tilde{p}_{hy} - \hat{p}_{ty})^2], \tag{22}$$

where r_0 is the area radius. Thus, $L_2(\tilde{\boldsymbol{x}}(k))$ is designed as

$$L_2(\tilde{\boldsymbol{x}}_h(k)) = \max\{0,\, g(\tilde{\boldsymbol{x}}_h(k))\}^2. \tag{23}$$

In (19), λ_1 and λ_2 are the tuned parameters to balance the weights of the cost terms.

The optimization problem in NMPC is finally established as

$$\min \quad J, \tag{24}$$

subjected to input constraints

$$\text{Input Cons. } |u(k)| \le u_m, \tag{25}$$

and dynamic equations

$$\text{Host UAV Kinematic Model: Eqs. (5) and (6)}, \tag{26}$$

$$\text{Intruder Kinematic Model: Eq. (9)}, \tag{27}$$

$$\text{Measurement Model: Eq. (13)}, \tag{28}$$

$$\text{EKF Dynamics: Eq. (15)}, \tag{29}$$

where u_m denotes the maximum heading velocity constraint.

The difficulty with the NMPC-based controller design is predicting EKF performance in the receding horizon window without knowing the real vision measurement that will happen in the future, that is, $\tilde{y}(k)$. To solve this issue, we use the intruder estimate $\hat{\boldsymbol{x}}_t(k)$ at the current moment to predict the intruder motion. Therefore, we can predict the vision measurement $\tilde{y}(k)$, and the EKF equations can be propagated as follows:

$$\tilde{z}_t(k|k) = \hat{z}_t(k|k). \tag{30}$$

4. Vision-Based SAA Approach in Return Phase

Once the intruder bypasses the host UAV, the SAA controller design for the avoidance phase will not work. For example, an optimization conflict may exist between the intruder motion estimation and trajectory tracking. The host UAV is even likely to turn around to chase the intruder for the optimal estimation performance. Thus, for the return phase, we need to design a new controller.

4.1. Switching criterion

We first need to determine a criterion when to switch between the two controllers. In this study, a switching criterion inspired by human driving behavior is employed (see Figure 4). We first define the nearest point on $\boldsymbol{\tau}$ with respect to the host UAV as $\boldsymbol{p}_\tau(k)$, that is, $\boldsymbol{p}_\tau(k) = \{\boldsymbol{p} \in \boldsymbol{\tau} | \min |\boldsymbol{p} - \boldsymbol{p}_h(k)|^2\}$. A line $\ell(x_l, y_l)$ is then defined to pass $\boldsymbol{p}_\tau(k)$ and $\boldsymbol{p}_h(k)$. When the intruder flies across ℓ, we consider it is time to switch between the avoidance phase and the return phase. Afterwards, the intruder is no longer considered a threat.

4.2. Host UAV kinematic model

Indeed, the return maneuver of the host UAV is purely a trajectory tracking problem. The host UAV can depend only on its navigation sensors to implement the return maneuver, and the monocular vision is actually not needed. In order to quickly track the predefined trajectory, the forward velocity $v_f(k)$ of the host UAV is also considered as a controllable input in this phase. Thus, we have

$$\boldsymbol{u}(k) = \begin{bmatrix} u_\varphi(k) \\ u_v(k) \end{bmatrix} := \begin{bmatrix} \varphi(k) \\ v_f(k) \end{bmatrix}. \tag{31}$$

https://doi.org/10.1017/S0263574719000158 Published online by Cambridge University Press

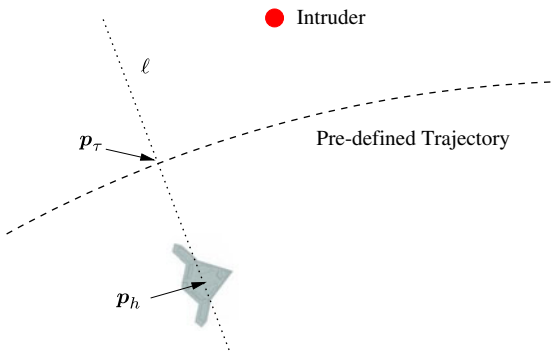


Fig. 4. Diagram of switching criterion.

The motion of host UAV is modeled as

$$\boldsymbol{P}_h(k+1) = \mathbf{I}_2 \boldsymbol{P}_h(k) + T \begin{bmatrix} \cos(\varphi(k)) \\ \sin(\varphi(k)) \end{bmatrix} v_f(k), \tag{32}$$

where $\mathbf{I}_2$ is the 2×2 identity matrix.

4.3. NMPC-based return maneuver

We still use NMPC in the return phase. The performance index of the controller is designed as

$$J = \sum_{i=0}^{N-1} L_3(\tilde{\boldsymbol{x}}_h(k+i)), \tag{33}$$

and

$$L_3(\tilde{\boldsymbol{x}}_h(k)) = |\tilde{\boldsymbol{x}}_h(k) - \boldsymbol{\tau}(k)|^2. \tag{34}$$

The optimization problem in NMPC is finally built as

$$\min \ \ J, \tag{35}$$

subjected to input constraints

$$\text{Input Cons. } |u_\varphi(k)| \le u_m \ \text{ and } \ |u_v(k)| \le u_n, \tag{36}$$

and dynamic equations

$$\text{Host UAV Kinematic Model: Eq. (32)}, \tag{37}$$

where u_m is the maximum heading velocity constraint and u_n represents the maximum forward speed.

Remark 2. The proposed approach provides a general framework for SAA operation. All the filter design, the NMPC performance index, and even the switch criterion are not unique and can be appropriately redesigned according to user requirements. For example, the use of predicted position uncertainty ellipse to evaluate estimation performance can be substituted by the other options discussed in ref. [34].

5. Simulation Results

We conduct extensive simulations to validate the proposed SAA approach.[1] The values of simulation parameters are listed in Table I. We assume the intruder is already confirmed as a real threat and the host UAV is on the predefined trajectory at the beginning of the SAA process. The intruder is noncooperative and flies at a constant forward speed. The EKF states are initialized with guess values. The simulations were performed on a standard desktop PC (2G Hz i5 CPU, 4G RAM) and

[1] Simulation videos are presented on https://pan.baidu.com/s/1bFb0sTQKSvhP7tZEaeazKw

https://doi.org/10.1017/S0263574719000158 Published online by Cambridge University Press

Table I. Parameters in simulation.

v_c (m/s)	T (s)	λ_1	λ_2	r_0 (m)	u_m (deg/s)	u_n (m/s)
12	0.2	100	50	50	5	18

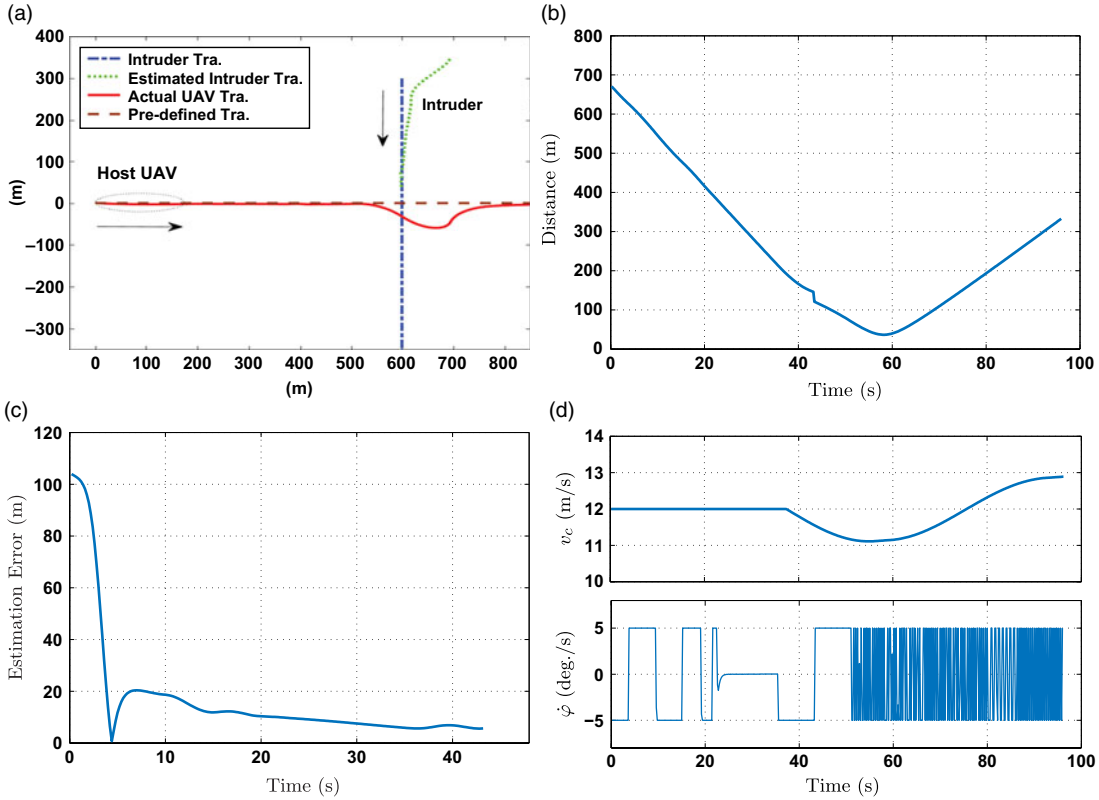


Fig. 5. Simulation results in Scenario 1. (a) Real avoidance trajectories. (b) Separation distance between the UAV and intruder. (c) EKF tracking error. (d) Controlled inputs of host UAV.

the MPC always ran faster than 10 Hz. For $\boldsymbol{v}_f$, we assign the Gaussian white noises with standard deviation 0.0001 rad/s, 0.00001 s^{-1}, 0.0001 rad, 0.0005 m^{-1} for each component, respectively. For v_h, we assume it is a Gaussian white noise with standard deviation 0.008 rad.

Three different SAA scenarios are investigated. Figure 5 shows the simulation results in Scenario 1. The trajectory of intruder is perpendicular to the predefined trajectory of the host UAV. Figure 5(a) demonstrates the real trajectories of the host UAV and the intruder, the predefined trajectory of the intruder, and the EKF estimated trajectory. The host UAV successfully avoids the intruder and returns to the predefined trajectory. Even with a larger initial deviation, the estimated EKF trajectory converges quickly to the real trajectory. From Figure 5(b), the minimum separation distance between the host UAV and the intruder is about 43 m. Figure 5(c) demonstrates the EKF tracking errors. At the beginning of the SAA process, the host UAV makes an aggressive maneuver to quickly reduce the initial EKF tracking errors. The portion is highlighted in the circle in Figure 5(a) and more clear results are observed in other two scenarios. Indeed, such a maneuver is necessary and beneficial to the vision-based SAA. Reference [34] has shown that increasing the angle separation between observations in angles-only navigation can improve the tracking performance of estimation filter. On the other side, the trajectory of host UAV is confined by the predefined trajectory. Therefore, the aggressive maneuver is reasonable by combing these two effects. The controller outputs are presented in Figure 5(d). The heading angle velocity and forward velocity of the host UAV are both bounded by the use of NMPC. The switch time between the avoidance controller and the return controller is approximately 38 s.

https://doi.org/10.1017/S0263574719000158 Published online by Cambridge University Press

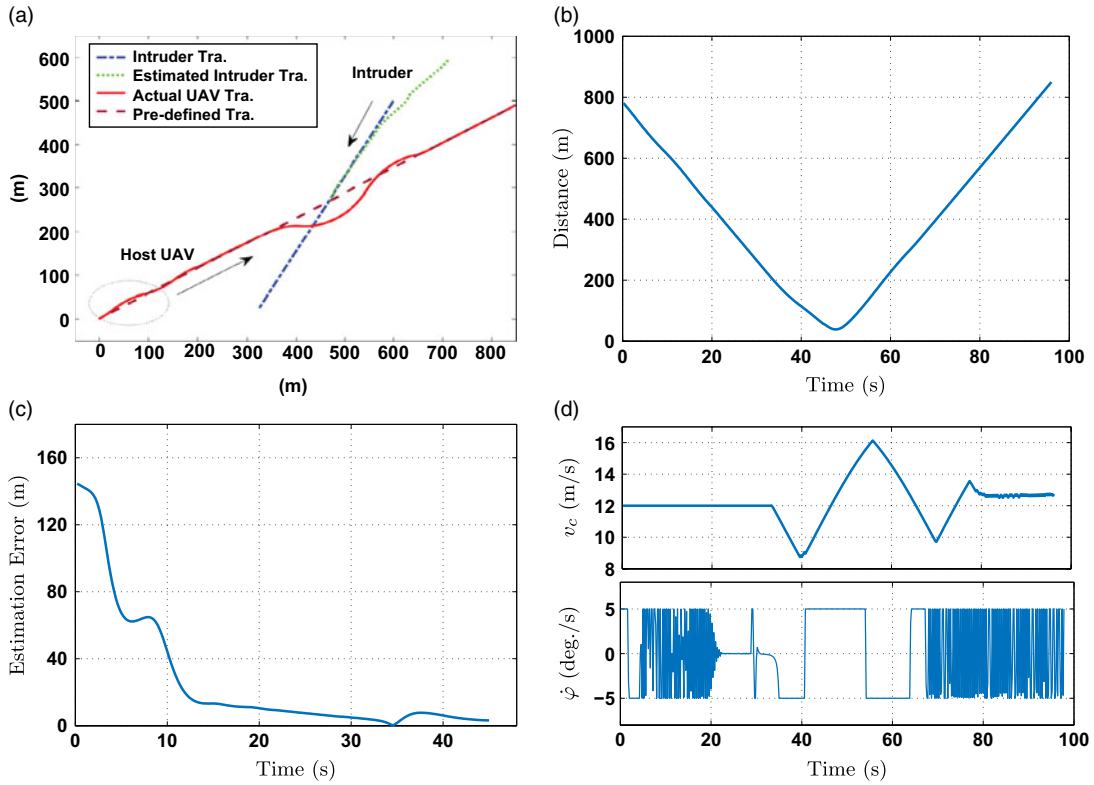


Fig. 6. Simulation results in Scenario 2. (a) Real avoidance trajectories. (b) Separation distance between the UAV and intruder. (c) EKF tracking error. (d) Controlled inputs of host UAV.

Figure 6 shows the simulation results in Scenario 2, where the trajectory of intruder is nearly head-on with a 30° intersection angle to the predefined trajectory of host UAV. We still observe satisfactory avoidance performance of the host UAV using the developed SAA approach. The EKF can also achieve a convergent estimation performance and estimate the motion of the intruder accurately. Figure 7 shows the simulation results in Scenario 3. In this case, the host UAV follows a curved predefined trajectory. Similarly, the host UAV effectively avoids the intruder and returns to the predefined trajectory. The EKF also performs a satisfactory estimation to obtain the motion of intruder. Under the proposed SAA approach, the host UAV achieves a simultaneous tradeoff between the trajectory tracking, intruder estimation, and intruder avoidance. The simulation results verified the effectiveness of the proposed SAA approach.

In order to further demonstrate the proposed approach, we conduct comparison results with different parameters in the performance index of NMPC for Scenario 1. Figure 8(a) and (b) illustrate the flying trajectories of host UAV and the areas of the predicted position uncertainty ellipse of EKF, respectively. From Figure 8(b), it is clear that increasing λ_1 will improve the estimation performance of target tracking filter. λ_2 almost has no influence on the target tracking filter. Figure 8(a) shows that increasing λ_2 may introduce more aggressive avoidance maneuver. However, the trend is very weak because the trajectories are also restricted by the filter and predefined trajectory.

6. Conclusion

In this paper, a novel monocular vision-based SAA approach for UAV was proposed by employing a NMPC design with an integrated target tracking filter. In the SAA approach, the designs of estimation, navigation, and control were combined in one framework. With the help of NMPC, the host UAV can simultaneously achieve reliable estimation performance, intruder avoidance, and predefined trajectory tracking. The effectiveness of the proposed approach was validated through extensive simulations. The work provided a general UAV SAA framework that can be readily extended to similar vision-based navigation and control studies.

https://doi.org/10.1017/S0263574719000158 Published online by Cambridge University Press

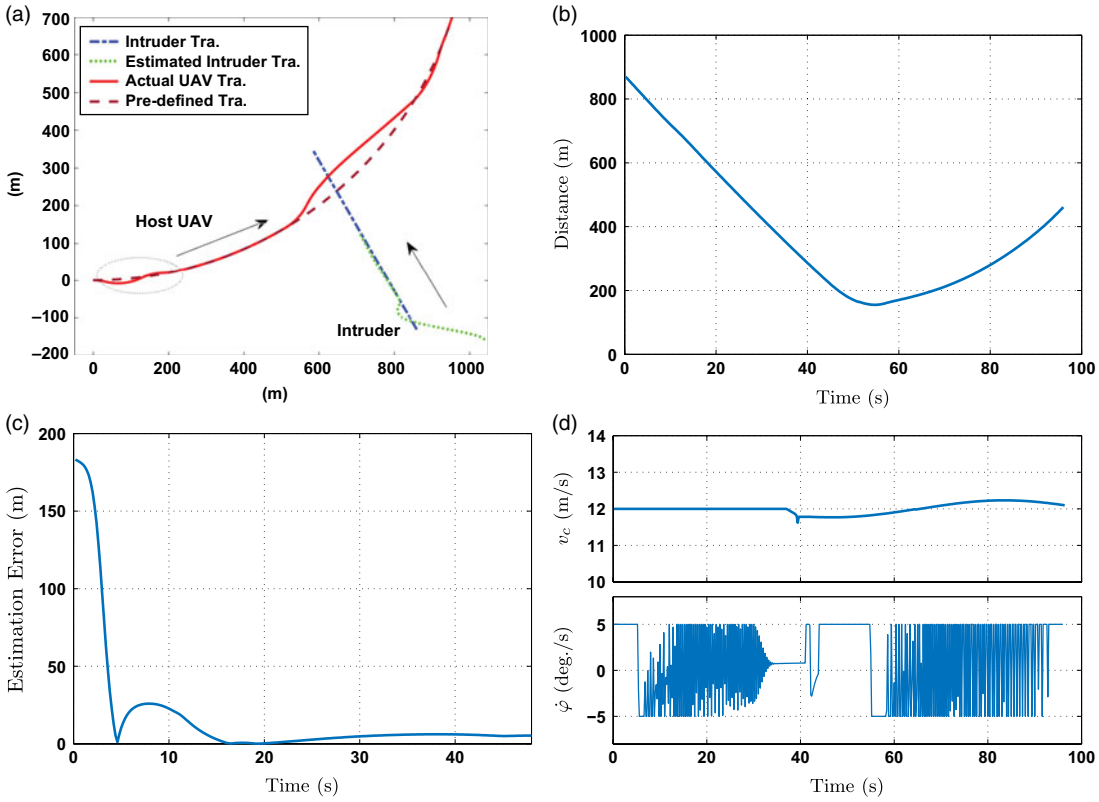


Fig. 7. Simulation results in Scenario 3. (a) Real avoidance trajectories. (b) Separation distance between the UAV and intruder. (c) EKF tracking error. (d) Controlled inputs of host UAV.

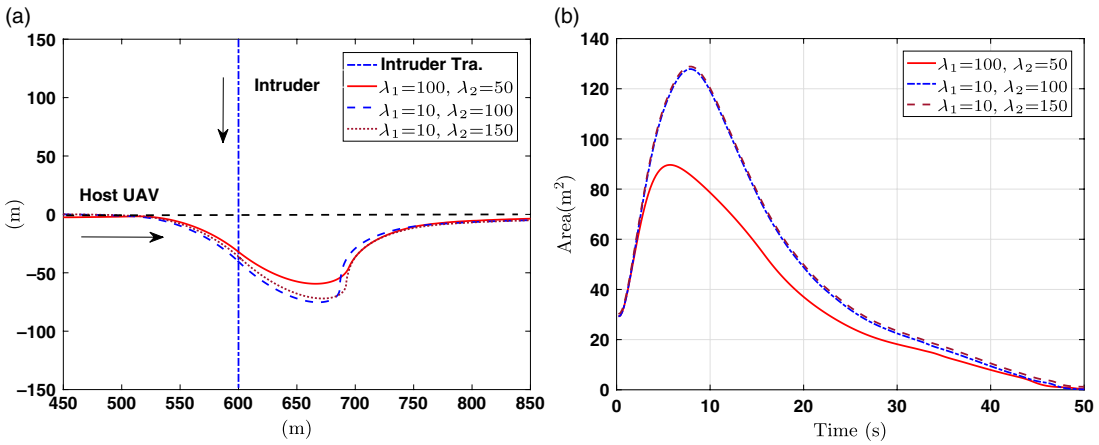


Fig. 8. Comparison results with different parameters in performance index for Scenario 1. (a) Trajectory comparison. (b) Area comparison of the predicted position uncertainty ellipse of EKF.

Acknowledgments

The authors thank Prof. Huiping Li of Northwestern Polytechnical University for his help on model predictive controller design and implementation. We are also grateful to H. Chang, Y. Hu, Y. Lu, and other members at the Research Center of Intelligent Robotics at Northwestern Polytechnical University. This work was partially supported by the National Science Foundation of China under grant 61873204, the Postdoctoral Science Foundation of China under grant 2017M620469 and 2018T111095, and State Key Laboratory of Robotics and System (HIT) under grant SKLRS-2018-KF-14.

https://doi.org/10.1017/S0263574719000158 Published online by Cambridge University Press

References

1. G. Oren and D. Yerach, "Fast and efficient visible trajectories planning for the Dubins UAV model in 3D built-up environments," *Robotica* **32**(1), 143–163 (2014).
2. X. Prats, L. Delgado, J. Ramirez, P. Royo and E. Pastor, "Requirements, issues, and challenges for sense and avoid in unmanned aircraft systems," *J. Aircr.* **49**(3), 677–687 (2012).
3. A. D. Zeitlin, " Sense and avoid capability development challenges," *IEEE Aerosp. Electron. Syst. Mag.* **25**(10), 27–32 (2010).
4. M. Melega, S. Lazarus, A. Savvaris and A. Tsourdos, " Multiple threats sense and avoid algorithm for static and dynamic obstacles," *J. Intell. Robot. Syst.* **77**(1), 215–228 (2015).
5. M. Wilson, D. Ryan, D. Bratanov, A. Wainwright, J. Ford, L. Cork and M. Brouckaert, "Flight test and evaluation of a prototype sense and avoid system onboard a scaneagle unmanned aircraft," *IEEE Aerosp. Electron. Syst. Mag.* **31**(9), 6–15 (2016).
6. X. Yu and Y. Zhang, "Sense and avoid technologies with applications to unmanned aircraft systems: Review and prospects," Prog. Aerosp. Sci. **74**, 152–166 (2015).
7. G. Fasano, D. Accado, A. Moccia and D. Moroney, "Sense and avoid for unmanned aircraft systems," *IEEE Aerosp. Electron. Syst. Mag.* **31**(11), 82–110 (2016).
8. H. C. Lee, "Implementation of collision avoidance system using TCAS II to UAVs," *IEEE Aerosp. Electron. Syst. Mag.* **21**(7), 8–13 (2006).
9. B. Stark, B. Stevenson and Y. Q. Chen, "ADS-B for small unmanned aerial systems: Case study and regulatory practices," **In:** *International Conference on Unmanned Aircraft Systems* (2013), pp. 152–159.
10. D. Accardo, G. Fasano, L. Forlenza and A. Moccia, "Flight test of a radar-based tracking system for UAS sense and avoid," *IEEE Trans. Aerosp. Electron. Syst.* **49**(2), 1139–1160 (2013).
11. M. Allistair, M. J. Rutherford, K. Michail and K. P. Valavanis, "UAV-borne X-band radar for collision avoidance," *Robotica* **32**(1), 97–114 (2013).
12. G. Fasano, D. Accardo, A. E. Tirri, A. Moccia and E. D. Lellis, "Radar/electro-optical data fusion for non-cooperative UAS sense and avoid," *Aerosp. Sci. Technol.* **46**(2), 436–450 (2015).
13. L. Chamberlain, S. Scherer and S. Singh, "Self-aware helicopters: Full-scale automated landing and obstacle avoidance in unmapped environments," Ahs Forum (2011).
14. C. Kownacki, "A concept of laser scanner designed to realize 3D obstacle avoidance for a fixed-wing UAV," *Robotica* **34**(2), 243–257 (2016).
15. S. Ramasamy, R. Sabatini, A. Gardi and J. Liu, "LIDAR obstacle warning and avoidance system for unmanned aerial vehicle sense-and-avoid," *Aerosp. Sci. Technol.* **55**, 344–358 (2016).
16. L. Mejias, J. Lai, J. J. Ford and P. O'Shea, "Demonstration of closed-loop airborne sense-and-avoid using machine vision," *IEEE Aerosp. Electron. Syst. Mag.* **27**(4), 4–7 (2012).
17. R. Hugo, S. Sergio and L. Rogelio, "Visual servoing applied to real-time stabilization of a multi-rotor UAV," *Robotica* **30**(7), 1203–1212 (2012).
18. H. Wang, D. Guo, X. Liang, W. Chen, G. Hu and K. K. Leang, "Adaptive vision-based leader-follower formation control of mobile robots," *IEEE Trans. Ind. Electron.* **64**(4), 2893–2902 (2017).
19. H. Wang, Y. Liu, W. Chen and Z. Wang, "A new approach to dynamic eye-in-hand visual tracking using nonlinear observers," *IEEE/ASME Trans. Mechatron.* **16**(2), 387–394 (2011).
20. L. Mejias, A. Mcfadyen and J. J. Ford, "Sense and avoid technology developments at Queensland University of Technology," *IEEE Aerosp. Electron. Syst. Mag.* **31**(7), 28–37 (2016).
21. Y. Min and Z. Min Z, "Unmanned aerial vehicle dynamic path planning in an uncertain environment," *Robotica* **33**(3), 611–621 (2015).
22. S. Suzuki, T. Ishii, Y. Aida, Y. Fujisawa, K. Iizuka and T. Kawamura, "Collision-free guidance control of small unmanned helicopter using nonlinear model predictive control," *Sice J. Control Meas. Syst. Integr.* **7**(6), 347–355 (2014).
23. X. Yang, L. M. Alvarez and T. Bruggemann, "A 3D collision avoidance strategy for UAVs in a non-cooperative environment," *J. Intell. Robot. Syst.* **70**(1–4), 315–327 (2013).
24. L. Yang, Q. Pan, C. Zhao and Y. Zhang, " Vision-based UAV collision avoidance with 2D dynamic safety envelope," *IEEE Aerosp. Electron. Syst. Mag.* **31**(7), 16–26 (2016).
25. S. Huh, S. Cho, Y. Jung and D. H. Shim, "Vision-based sense-and-avoid framework for unmanned aerial vehicles," *IEEE Trans. Aerosp. Electron. Syst.* **51**(4), 3427–3439 (2015).
26. P. J. Nordlund and F. Gustafsson, "Probabilistic noncooperative near mid-air collision avoidance," *IEEE Trans. Aerosp. Electron. Syst.* **47**(2), 1265–1276 (2011).
27. H. Yu and R. W. Beard, "Vision-based local-level frame mapping and planning in spherical coordinates for miniature air vehicles," *IEEE Trans. Control Syst. Technol.* **21**(3), 695–703 (2013).
28. S. C. Nardone and V. J. Aidala, "Observability criteria for bearings-only target motion analysis," *IEEE Trans. Aerosp. Electron. Syst. AES* **17**(2), 162–166 (1981).
29. V. J. Aidala, "Kalman filter behavior in bearings-only tracking applications," *IEEE Trans. Aerosp. Electron. Syst.* **15**(1), 29–39 (1979).
30. V. J. Aidala and S. E. Hammel, "Utilization of modified polar coordinates for bearings-only tracking," *IEEE Trans. Autom. Control* **28**(3), 283–294 (1983).
31. J. M. Passerieux and D. V. Cappel, "Optimal observer maneuver for bearings-only tracking," *IEEE Trans. Aerosp. Electron. Syst.* **34**(3), 777–788 (1998).

https://doi.org/10.1017/S0263574719000158 Published online by Cambridge University Press

32. S. DiCairano, H. Park and I. Kolmanovsky, "Model predictive control approach for guidance of spacecraft rendezvous and proximity maneuvering," *Int. J. Robust Nonlinear Control* **22**(12), 1398–1427 (2012).
33. A. Weiss, M. Baldwin, R. S. Erwin and I. Kolmanovsky, "Model predictive control for spacecraft rendezvous and docking: Strategies for handling constraints and case studies," *IEEE Trans. Control Syst. Technol.* **23**(4), 1638–1647 (2015).
34. S. Ponda, R. Kolacinski and E. Frazzoli, "Trajectory optimization for target localization using small unmanned aerial vehicles," **In:** *AIAA Guidance, Navigation, and Control Conference* (2009).

https://doi.org/10.1017/S0263574719000158 Published online by Cambridge University Press